

BLIND DIRECTION OF ARRIVAL ESTIMATION OF COHERENT SOURCES USING MULTI-INVARIANCE PROPERTY

X. Zhang, J. Yu, G. Feng, and D. Xu

Electronic Engineering Department
Nanjing University of Aeronautics & Astronautics
Nanjing 210016, China

Abstract—Blind direction of arrival (DOA) estimation algorithms of coherent sources using multi-invariance property is presented in this paper. ESPRIT-like algorithm in [23] can estimate DOA of coherent signal, but its performance is without satisfaction. We reconstruct the received signal to form data model with multi-invariance property, and then multi-invariance ESPRIT and multi-invariance MUSIC algorithms for coherent DOA estimation are proposed in this paper. Our proposed algorithms can resolve the DOAs of coherent signals. They have much better DOA estimation performance than ESPRIT-like algorithm. Meanwhile they identify more DOAs than ESPRIT-like algorithm. The simulation results demonstrate their validity.

1. INTRODUCTION

Antenna array has been used in many fields such as radar, sonar, communications, seismic data processing, etc. [1–12]. The directions-of-arrival (DOA) estimation [13–18] of signals impinging on an array of sensors is a fundamental problem in array processing, and many methods have been proposed for its solution. Eigen-decomposition-based methods, including multiple signal classification (MUSIC) and estimation of signal parameters via rotational invariance techniques (ESPRIT), have high resolution DOA estimation performance, but they fail to work in coherent signal condition. Some smoothing methods including spatial smoothing techniques [18, 19], subspace smoothing techniques [21], temporal smoothing techniques [22] etc. were proposed to resolve this coherent problem. But these methods are all at the cost of a reduction in array aperture, the number of resolved sources is restricted within the number of reduced array.

Some higher-order cumulants based methods [24, 25] and third-order cyclic moment method [22] can resolve coherent DOA estimation, but the required number of snapshots is too large and the complexity is relatively high; they also require the signal statistic characteristic. [26] derives a large-sample maximum likelihood estimator for coherent DOA estimation, which may be difficult to realize. Some special array structures [23, 27] are used for coherent DOA estimation. In [23], a coherent DOA estimation was presented from another point of view, which reconstructed a special antenna array model based on the Toeplitz matrix whose rank is only related to the DOA of signals and cannot be affected by the coherency between them. EPSPIT method is used to coherent DOA estimation, but its DOA estimation performance is without satisfaction. Also, ESPRIT-like algorithm [23] requires stronger conditions in terms of the number of sensors, $N > 2P + 1$, where N, P are the numbers of antennas and sources, respectively.

Improved DOA estimation algorithms of coherent signal are investigated in this paper. Our proposed algorithms, which employ multi-invariance property, have much better DOA estimation performance than ESPRIT-like algorithm and identify more DOAs than ESPRIT-like algorithm. Our proposed algorithm can overcome the shortcomings of EPSPIT-like method.

This paper is structured as follows. Section 2 develops data model. Section 3 deals with algorithmic issues. Section 4 presents simulation results, and Section 5 summarizes our conclusions.

Denote: We denote by $(\cdot)^*$ the complex conjugation, by $(\cdot)^T$ the matrix transpose, and by $(\cdot)^H$ the matrix conjugate transpose. The notation $(\cdot)^+$ refers to the Moore-Penrose inverse (pseudo inverse). $\|\cdot\|_F$ stands for Forbenius norm.

2. DATA MODEL

A uniform linear array (ULA) with spacing d is considered in this paper. The structure of uniform linear array is shown in Fig. 1. The received signal of antenna array containing $N(N = 2M + 1)$ elements is shown

$$\mathbf{X} = \mathbf{A}\mathbf{S} + \mathbf{N}_0 \quad (1)$$

where $\mathbf{S} = [\mathbf{s}_1 \cdots \mathbf{s}_1 \mathbf{s}_{L+1} \cdots \mathbf{s}_p]$. We suppose that the first L signals are mutually coherent, while the others are independent of the first signals. \mathbf{N}_0 is the received noise. \mathbf{A} is the direction matrix. $\mathbf{A} = [\mathbf{a}(\theta_1) \mathbf{a}(\theta_2) \cdots \mathbf{a}(\theta_p)]$, where $\mathbf{a}(\theta_p) = [e^{j2\pi dM \sin \theta_p / \lambda} \cdots 1 \cdots e^{-j2\pi dM \sin \theta_p / \lambda}]^T$, and λ is wavelength.

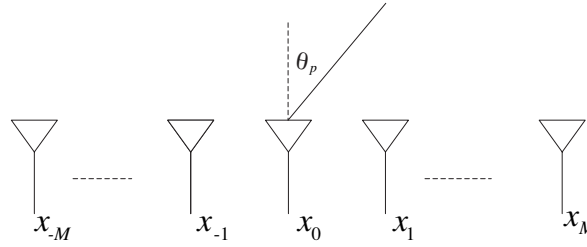


Figure 1. The structure of array antennas.

The covariance matrix of the received signal is $\mathbf{R}_{xx} = E\{\mathbf{X}\mathbf{X}^H\}$, where $E\{\cdot\}$ stands for the expectation. According to [23], the element of \mathbf{R}_{xx} can be expressed as

$$r(m, n) = \sum_{i=1}^P d_{m,i} e^{j2\pi d n \sin \theta_i / \lambda} + \sigma_n^2 \delta_{m,n},$$

$$m, n = -M, \dots, 0, \dots, M \quad (2)$$

where $d_{m,i}$ is shown in [23].

We collect data and form the following Toeplitz matrices with $(M+1) \times (M+1)$

$$\mathbf{R}(m) = \begin{bmatrix} r(m, 0) & r(m, 1) & \cdots & r(m, M) \\ r(m, -1) & r(m, 0) & \cdots & r(m, M-1) \\ \vdots & \vdots & \ddots & \vdots \\ r(m, -M) & r(m, -M+1) & \cdots & r(m, 0) \end{bmatrix},$$

$$m = -M, \dots, 0, \dots, M$$

$$= \mathbf{A}_r \mathbf{D}(m) \mathbf{A}_r^H + \mathbf{N}_m \quad (3)$$

where $\mathbf{D}(m) = \text{diag}\{d_{m,1} \ d_{m,2} \ \cdots \ d_{m,P}\} \in \mathbb{C}^{P \times P}$, \mathbf{N}_m is the noise component.

$\mathbf{A}_r = [\mathbf{a}_r(\theta_1) \ \mathbf{a}_r(\theta_2) \ \cdots \ \mathbf{a}_r(\theta_p)] \in \mathbb{C}^{M+1 \times P}$, and $\mathbf{a}_r(\theta_p) = [1 \ e^{-j(2\pi/\lambda)d \sin \theta_p} \ \cdots \ e^{-j(2\pi/\lambda)dM \sin \theta_p}]^T$.

Define a matrix \mathbf{H} as

$$\mathbf{H} = \begin{bmatrix} d_{-M,1} & d_{-M,2} & \cdots & d_{-M,P} \\ \vdots & \vdots & \ddots & \vdots \\ d_{0,1} & d_{0,2} & \cdots & d_{0,P} \\ \vdots & \vdots & \ddots & \vdots \\ d_{M,1} & d_{M,2} & \cdots & d_{M,P} \end{bmatrix} \in \mathbb{C}^{2M+1 \times P} \quad (4)$$

Define $\mathbf{R}_k = \mathbf{R}(m)$, for $k = m + M + 1$, $k = 1, 2, \dots, 2M + 1$ and $m = -M, \dots, 0, \dots, M$. \mathbf{R}_k is shown

$$\mathbf{R}_k = \mathbf{A}_r \text{diag}_k(\mathbf{H}) \mathbf{A}_r^H + \mathbf{N}_k, \quad k = 1, 2, \dots, 2M + 1 \quad (5)$$

where $\text{diag}_k(\cdot)$ extract the k th row of its matrix argument and construct a diagonal matrix out of it. \mathbf{A}_r is a matrix with Vandermode characteristic, so we can use ESPRIT method [28] to estimate DOA.

According to Eq. (5), we get

$$\begin{bmatrix} \mathbf{R}_1 \\ \mathbf{R}_2 \\ \vdots \\ \mathbf{R}_{2M+1} \end{bmatrix} = \begin{bmatrix} \mathbf{A}_r \text{diag}_1(\mathbf{H}) \\ \mathbf{A}_r \text{diag}_2(\mathbf{H}) \\ \vdots \\ \mathbf{A}_r \text{diag}_{2M+1}(\mathbf{H}) \end{bmatrix} \mathbf{A}_r^H + \begin{bmatrix} \mathbf{N}_1 \\ \mathbf{N}_2 \\ \vdots \\ \mathbf{N}_{2M+1} \end{bmatrix} \quad (6)$$

The noiseless signal in Eq. (5) can be denoted as trilinear model [29], which has been used in [30–34].

$$x_{m,n,k} = \sum_{p=1}^P a_{m,p} a_{n,p}^* h_{k,p},$$

$$m = 1, \dots, M+1; n = 1, \dots, M+1; k = 1, 2, \dots, 2M+1 \quad (7)$$

where $a_{m,p}$ stands for (m, p) element of matrix \mathbf{A}_r ; $h_{k,p}$ stands for (k, p) element of matrix \mathbf{H} . $\mathbf{A}_r \text{diag}_k(\mathbf{H}) \mathbf{A}_r^H$, $k = 1, 2, \dots, 2M - 1$, can be interpreted as slicing the trilinear model in a series of slices (2-D data or matrix) along the antenna direction. The symmetry of trilinear model in Eq. (7) allows other matrix system rearrangements which can be interpreted as slicing the trilinear model along different directions. In particular

$$\mathbf{Y}_m = \mathbf{A}_r^* \text{diag}_m(\mathbf{A}_r) \mathbf{H}^T, \quad m = 1, 2, \dots, M + 1 \quad (8)$$

where Eq. (8) can be regarded as the reconstructing signal of Eq. (5).

3. BLIND DOA ESTIMATION OF COHERENT SOURCES USING MULTI-INVARIANCE PROPERTY

3.1. Multi-invariance ESPRIT (MI-ESPRIT) Algorithm for Coherent DOA Estimation

According to Eq. (8), we form the following matrix.

$$\mathbf{Y} = \begin{bmatrix} \mathbf{Y}_1 \\ \mathbf{Y}_2 \\ \vdots \\ \mathbf{Y}_{M+1} \end{bmatrix} = \begin{bmatrix} \mathbf{A}_r^* \text{diag}_1(\mathbf{A}_r) \\ \mathbf{A}_r^* \text{diag}_2(\mathbf{A}_r) \\ \vdots \\ \mathbf{A}_r^* \text{diag}_{M+1}(\mathbf{A}_r) \end{bmatrix} \mathbf{H}^T = \begin{bmatrix} \mathbf{A}_r^* \\ \mathbf{A}_r^* \Phi \\ \vdots \\ \mathbf{A}_r^* \Phi^M \end{bmatrix} \mathbf{H}^T \quad (9)$$

where $\Phi = \text{diag}[e^{-j(2\pi/\lambda)d\sin\theta_1}, e^{-j(2\pi/\lambda)d\sin\theta_2}, \dots, e^{-j(2\pi/\lambda)d\sin\theta_p}]$, which is called the rotation matrix. So we can use multi-invariance ESPRIT [35] to estimate DOAs.

For Eq. (9), $\mathbf{R}_Y = \mathbf{Y}\mathbf{Y}^H$. We denote the matrix containing the eigenvectors $\{\mathbf{f}_p\}_{p=1}^P$ associated with the P largest eigenvalues of \mathbf{R}_Y by \mathbf{E}

$$\mathbf{E} = \begin{bmatrix} \mathbf{A}_r^* \\ \mathbf{A}_r^*\Phi \\ \vdots \\ \mathbf{A}_r^*\Phi^M \end{bmatrix} \mathbf{T} \quad (10)$$

where \mathbf{T} is a $P \times P$ full-rank matrix.

According to (10), we define \mathbf{E}_1 and \mathbf{E}_2

$$\mathbf{E}_1 = \begin{bmatrix} \mathbf{A}_r^* \\ \mathbf{A}_r^*\Phi \\ \vdots \\ \mathbf{A}_r^*\Phi^{M-1} \end{bmatrix} \mathbf{T} \quad (11)$$

$$\mathbf{E}_2 = \begin{bmatrix} \mathbf{A}_r^*\Phi \\ \mathbf{A}_r^*\Phi^2 \\ \vdots \\ \mathbf{A}_r^*\Phi^M \end{bmatrix} \mathbf{T} \quad (12)$$

According to Eq. (11) and Eq. (12),

$$\mathbf{E}_2 = \begin{bmatrix} \mathbf{A}_r^* \\ \mathbf{A}_r^*\Phi \\ \vdots \\ \mathbf{A}_r^*\Phi^{M-1} \end{bmatrix} \Phi \mathbf{T} = \begin{bmatrix} \mathbf{A}_r^* \\ \mathbf{A}_r^*\Phi \\ \vdots \\ \mathbf{A}_r^*\Phi^{M-1} \end{bmatrix} \mathbf{T} \mathbf{T}^{-1} \Phi \mathbf{T} = \mathbf{E}_1 \mathbf{T}^{-1} \Phi \mathbf{T} \quad (13)$$

Define $\Psi = \mathbf{T}^{-1} \Phi \mathbf{T}$. Eq. (13) becomes $\mathbf{E}_2 = \mathbf{E}_1 \Psi$, and then $\Psi = \mathbf{E}_1^+ \mathbf{E}_2$. Because Ψ has the same eigenvalues as Φ , we use eigenvalue decomposition (EVD) for Ψ to get $e^{-j(2\pi/\lambda)d\sin\theta_p}$, $p = 1, 2, \dots, P$, and then estimate DOA θ_p , $p = 1, 2, \dots, P$.

It should be pointed out that ESPRIT-like algorithm [17] requires stronger conditions in terms of the number of sensors, $N > 2P + 1$, where N , P are the numbers of antennas and sources, respectively. Our proposed algorithm has no this limitation. Exploiting multiple invariance characteristic in Eq. (11) and Eq. (12), it easy to determine the maximum number of users K_{\max} which MI-ESPRIT algorithm can

detect. It is clear $K_{\max} = M(M + 1)$ ($N = 2M + 1$). We also consider the number of sources $K \leq N$. So the number of sources which MI-ESPRIT can identify $K \leq \min\{M(M + 1), N\}$.

3.2. Multi-invariance MUSIC (MI-MUSIC) Algorithm for Coherent DOA Estimation

We also use multi-invariance MUSIC [36] to estimate coherent DOA. In [36], DOAs of uncorrelated sources are estimated with multi-invariance MUSIC, but herein we employ multi-invariance MUSIC to estimate DOAs of coherent sources. Equation (10) is also denoted as

$$\mathbf{E} = \Lambda \mathbf{T} \quad (14)$$

where \mathbf{T} is a $P \times P$ full-rank matrix. Λ is

$$\Lambda = \begin{bmatrix} \mathbf{A}_r^* \\ \mathbf{A}_r^* \Phi \\ \vdots \\ \mathbf{A}_r^* \Phi^M \end{bmatrix} = [\mathbf{a}_1 \otimes \beta_1, \mathbf{a}_2 \otimes \beta_2, \dots, \mathbf{a}_p \otimes \beta_p] \quad (15)$$

where \mathbf{a}_p is the p th column of the matrix \mathbf{A}_r . β_p is the p th column of the matrix \mathbf{A}_r^* . $\mathbf{a}_p \otimes \beta_p$ denotes Kronecker product.

According to Eq. (14), $\Lambda = \mathbf{E} \mathbf{T}^{-1}$, and then minimizing the signal subspace fitting, $\hat{\mathbf{T}}, \hat{\Lambda} = \arg \min_{\mathbf{T}, \Lambda} \left\| \Lambda - \hat{\mathbf{E}} \mathbf{T}^{-1} \right\|_F^2$, which is also denoted as

$$\hat{\mathbf{T}}, \hat{\Lambda} = \arg \min tr(\Lambda^H \Pi_{\hat{\mathbf{E}}}^\perp \Lambda) \quad (16)$$

where $tr(\cdot)$ denotes the sum of the elements of the principal diagonal of the matrix. $\Pi_{\hat{\mathbf{E}}}^\perp = \mathbf{I} - \hat{\mathbf{E}}(\hat{\mathbf{E}}^H \hat{\mathbf{E}})^{-1} \hat{\mathbf{E}}^H$, and \mathbf{I} is a $(M + 1) \times (M + 1)$ identity matrix. According to Eq. (15), the minimization of Eq. (16) becomes

$$\hat{\mathbf{a}}_p, \hat{\beta}_p = \arg \min_{\mathbf{a}_p, \beta_p} \sum_{p=1}^P (\mathbf{a}_p \otimes \beta_p)^H \Pi_{\hat{\mathbf{E}}}^\perp (\mathbf{a}_p \otimes \beta_p) \quad (17)$$

The minimization for Eq. (17) can be attained by finding the P deepest minima of the following criterion.

$$\begin{aligned} \mathbf{V}(\theta, \beta) &= (\mathbf{a}(\theta) \otimes \beta)^H \Pi_{\hat{\mathbf{E}}}^\perp (\mathbf{a}(\theta) \otimes \beta) \\ &= \beta^H (\mathbf{a}(\theta) \otimes \mathbf{I})^H \Pi_{\hat{\mathbf{E}}}^\perp (\mathbf{a}(\theta) \otimes \mathbf{I}) \beta \\ &= \beta^H \mathbf{Q}(\theta) \beta \end{aligned} \quad (18)$$

where $\mathbf{a}(\theta) = [1 \ e^{-j(2\pi/\lambda)d\sin\theta} \ \dots \ e^{-j(2\pi/\lambda)dM\sin\theta}]^T \in \mathbb{C}^{(M+1) \times 1}$; $\mathbf{Q}(\theta) = (\mathbf{a}(\theta) \otimes \mathbf{I})^H \Pi_{\hat{\mathbf{e}}}^\perp (\mathbf{a}(\theta) \otimes \mathbf{I})$; $\beta \in \mathbb{C}^{(M+1) \times 1}$. \mathbf{I} is the $(M+1) \times (M+1)$ identity matrix. A constraint $\mathbf{e}^T \beta = 1$, where $\mathbf{e} = [1, 0, \dots, 0]^T \in \mathbb{R}^{(M+1) \times 1}$, is added to eliminate the trivial solution $\beta = 0$. The DOA θ_p , $p = 1, 2, \dots, P$, are estimated via a 1-D search. The solution for θ_p is

$$\hat{\theta}_p = \arg \max_{\theta} \mathbf{e}^T \mathbf{Q}^{-1}(\theta) \mathbf{e} \quad (19)$$

Searching $\theta \in [0, 360^\circ]$, we find the P largest peak of the (1, 1) element of $\mathbf{Q}^{-1}(\theta)$. The P largest peak should correspond to DOA θ_p , $p = 1, 2, \dots, P$.

3.3. Complexity Analysis

In contrast to ESPRIT, our algorithms have a larger computational load, which is usually dominated by formation of the covariance matrix and calculation of EVD.

For MI-ESPRIT algorithm, the computational complexity of formation of the covariance matrix is $O((M+1)^4(2M+1))$; calculation of its eigen decomposition requires $O((M+1)^6)$; and eigen value decomposition for Ψ requires $O(P^3)$. The major computational complexity of MI-ESPRIT is $O((M+1)^4(2M+1) + (M+1)^6 + P^3)$, while ESPRIT requires $O((M+1)^2(2M+1)P + (M+1)^3 + P^3)$.

For MI-MUSIC algorithm, the computational complexity of formation of the covariance matrix is $O((M+1)^4(2M+1))$ and calculation of its eigen decomposition requires $O((M+1)^6)$. For MI-MUSIC, which employs a 1-D criterion that must be searched for P local maximum, the computational load is determined by the complexity of evaluating the criterion for each θ . MI-MUSIC requires the formation of the matrix $\mathbf{Q}(\theta)$ for each θ , which is an $O((M+1)^4)$ operation, followed by calculation of the (1, 1) element of $\mathbf{Q}^{-1}(\theta)$, which requires $O((M+1)^4)$.

4. SIMULATION RESULTS

Let $\mathbf{R}_k = \mathbf{A}_r \text{diag}_k(\mathbf{H}) \mathbf{A}_r^H + \mathbf{N}_k$ be the received noisy data, for $k = 1, 2, \dots, 2M-1$, where \mathbf{N}_k are the additive white Gaussian noise (AWGN) matrices. We define signal to noise ratio (SNR)

$$\text{SNR} = 10 \log_{10} \frac{\sum_{k=1}^{2M+1} \|\mathbf{A}_r \text{diag}_k(\mathbf{H}) \mathbf{A}_r^H\|_F^2}{\sum_{k=1}^{2M+1} \|\mathbf{N}_k\|_F^2} \quad (20)$$

A uniform linear array with $N = 11$ ($N = 2M + 1$, then $M = 5$) sensors is used in this simulation, and there are three signals $s_i(t) = \rho_i e^{j(2\pi ft + \phi_i)}$, $i = 1, 2, 3$, impinging on a uniform linear array at $\theta_1 = 10^\circ$, $\theta_2 = 20^\circ$, $\theta_3 = 30^\circ$ respectively. ρ_i and ϕ_i stand for the power and the initial phase of signal, respectively. The second signal is the duplicate of the first signal, and the third signal is independent of first signal. The element spacing d is $\lambda/2$. Define $MSE = \frac{1}{1000} \sum_m^{1000} |\theta_m - \theta_0|^2$, where θ_m is the estimated DOA of the m th simulation, θ_0 is the perfect DOA. We present Monte Carlo simulations that assess DOA estimation performance of the proposed algorithms. The number of Monte Carlo trials is 1000.

Figure 2 and Fig. 3 show the DOA estimation of MI-ESPRIT and MI-MUSIC algorithm at 30 dB. From Fig. 2–Fig. 3, we find that our proposed algorithms (MI-ESPRIT and MI-MUSIC algorithm) have better coherent DOA estimation performance.

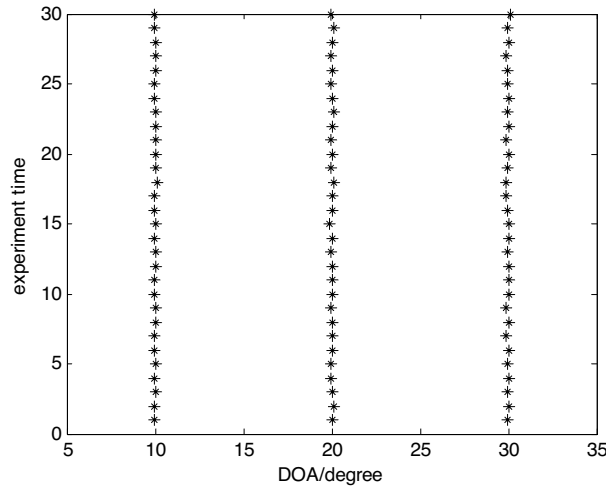


Figure 2. DOA estimation performance of MI-ESPRIT at SNR = 30 dB.

We compare our algorithms with ESPRIT [23]. Their DOA estimation performance comparisons under different SNR are shown in Figs. 4–6. Fig. 4 shows the MSE of the estimate of $\theta_1 = 10^\circ$ versus SNR, and from Fig. 4 we find that MI-ESPRIT algorithm has much better DOA estimation performance than ESPRIT-like algorithm. The DOA estimation performance of MI-ESPRIT algorithm is about 9 dB better than ESPRIT-like algorithm. MI-MUSIC algorithm has about 1 dB gain over MI-ESPRIT, and about 10 dB over ESPRIT algorithm. Fig. 5 and Fig. 6 present $\theta_2 = 20^\circ$ and $\theta_3 = 30^\circ$

estimation performance, respectively. From Fig. 5 and Fig. 6, we find that MI-ESPRIT algorithm has much better DOA estimation performance than ESPRIT-like algorithm. MI-MUSIC algorithm has better DOA estimation performance than MI-ESPRIT. MI-ESPRIT and MI-MUSIC algorithms have better coherent DOA estimation than ESPRIT, because MI-ESPRIT and MI-MUSIC algorithms utilize fully multi-invariance structure.

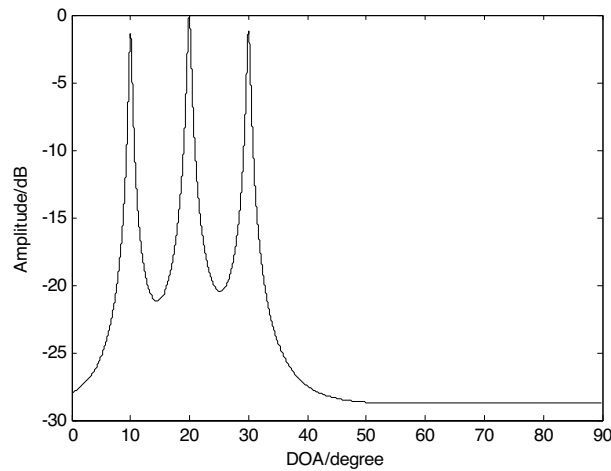


Figure 3. DOA estimation performance of MI-MUSIC at SNR = 30 dB.

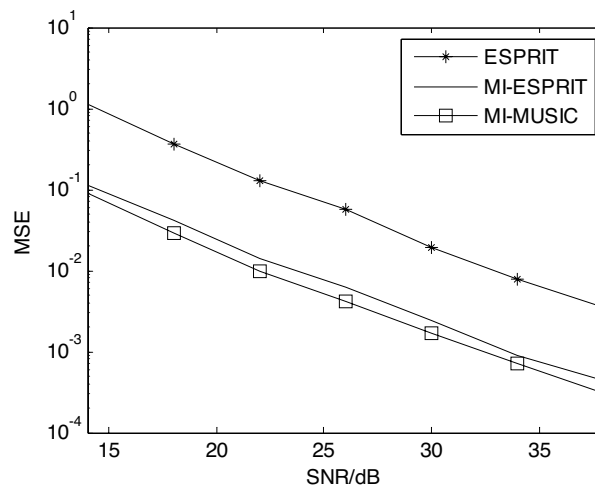


Figure 4. MSE of the estimate of $\theta_1 = 10^\circ$ versus SNR.

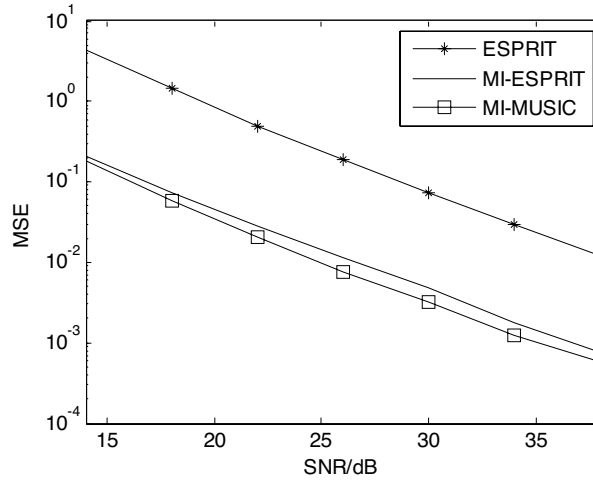


Figure 5. MSE of the estimate of $\theta_2 = 20^\circ$ versus SNR.

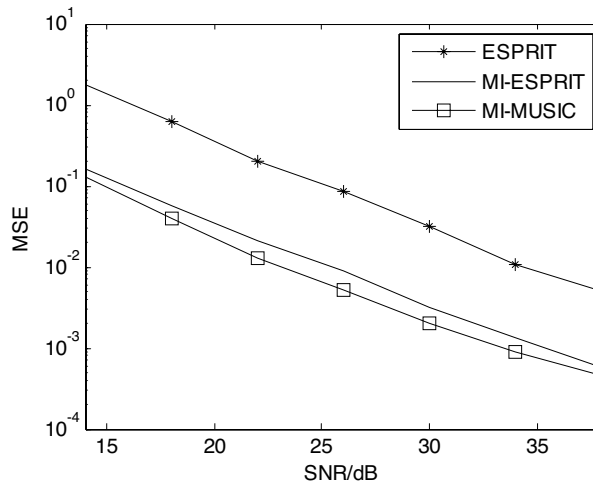


Figure 6. MSE of the estimate of $\theta_3 = 30^\circ$ versus SNR.

As we mentioned above, ESPRIT-like algorithm in [23] only works well when $P < M + 1$. When $P \geq M + 1$, ESPRIT-like algorithm fails to work. Our proposed algorithm has no this limitation. Suppose there are 6 signals impinging on a uniform linear array with $N = 11$ ($N = 2M + 1$, then $M = 5$) sensors at $\theta_1 = 10^\circ$, $\theta_2 = 20^\circ$, $\theta_3 = 30^\circ$, $\theta_4 = 40^\circ$, $\theta_5 = 50^\circ$, $\theta_6 = 60^\circ$, respectively. The second signal is the duplicate of the first signal, while other signals are independent

of first signal. Fig. 7 shows the DOA estimation of MI-ESPRIT at 38 dB with 30 independent trials. Fig. 8 presents the DOA estimation performance of MI-MUSIC algorithm. From Figs. 7–8, we conclude that our proposed algorithms have better coherent DOA estimation performance with larger source number. They identify more DOAs than ESPRIT-like algorithm.

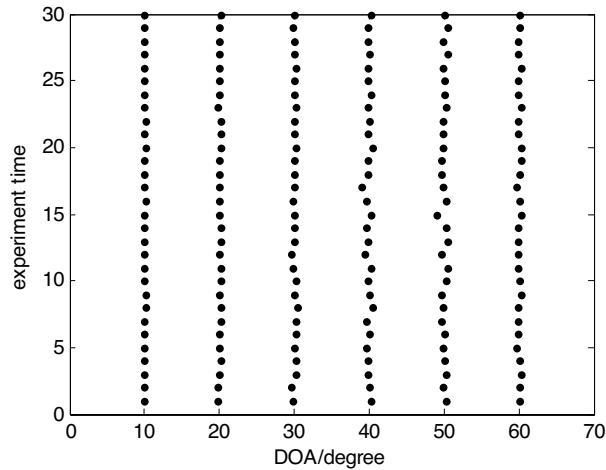


Figure 7. DOA estimation performance of MI-ESPRIT at SNR = 38 dB.

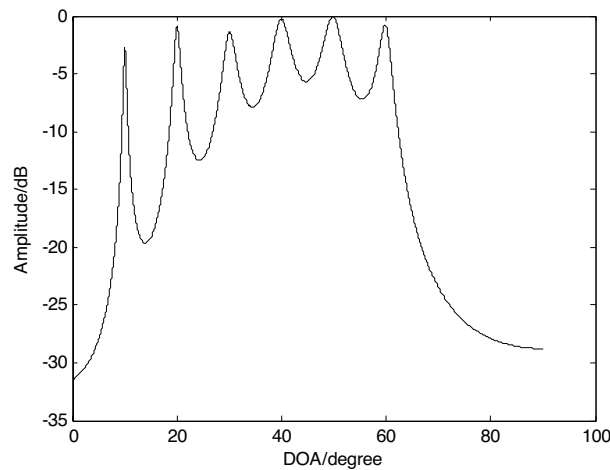


Figure 8. DOA estimation performance of MI-MUSIC at SNR = 38 dB.

5. CONCLUSIONS

We reconstruct the received signal to form data model with multi-invariance property, so multi-invariance ESPRIT and multi-invariance MUSIC algorithms for coherent DOA estimation are proposed in this paper. Our proposed algorithm can resolve the DOAs of coherent signals. Our proposed algorithm has much better DOA estimation performance than ESPRIT-like algorithm, meanwhile they identify more DOAs than ESPRIT-like algorithm. Multi-invariance MUSIC algorithm has the better DOA estimation performance than multi-invariance ESPRIT algorithm, but its computational complexity is larger than multi-invariance ESPRIT algorithm.

ACKNOWLEDGMENT

This work is supported by China NSF Grants (60801052) and Jiangsu NSF Grants (BK2007192). The authors wish to thank the anonymous reviewers for their valuable suggestions on improving this paper.

REFERENCES

1. Qu, Y., G. Liao, S.-Q. Zhu, and X.-Y. Liu, "Pattern synthesis of planar antenna array via convex optimization for airborne forward looking radar," *Progress In Electromagnetics Research*, PIER 84, 1–10, 2008.
2. Yang, Y., Y. Wang, and A. E. Fathy, "Design of compact Vivaldi antenna arrays for UWB see through wall applications," *Progress In Electromagnetics Research*, PIER 82, 401–418, 2008.
3. Guney, K. and M. Onay, "Amplitude-only pattern nulling of linear antenna arrays with the use of bees algorithm," *Progress In Electromagnetics Research*, PIER 70, 21–36, 2007.
4. Liang, L., B. Li, S.-H. Liu, and C.-H. Liang, "A study of using the double negative structure to enhance the gain of rectangular waveguide antenna arrays," *Progress In Electromagnetics Research*, PIER 65, 275–286, 2006.
5. Abouda, A., H. M. El-Sallabi, and S. G. Häggman, "Effect of antenna array geometry and ULA azimuthal orientation on MIMO channel properties in urban city street grid," *Progress In Electromagnetics Research*, PIER 64, 257–278, 2006.
6. Mouhamadou, M., P. Vaudon, and M. Rammal, "Smart antenna array patterns synthesis: Null steering and multi-user

- beamforming by phase control,” *Progress In Electromagnetics Research*, PIER 60, 95–106, 2006.
7. Gustafsson, M., “RCS reduction of integrated antenna arrays with resistive sheets,” *Journal of Electromagnetic Waves and Applications*, Vol. 20, No. 1, 27–40, 2006.
 8. Fu, Y.-Q., Q.-R. Zheng, Q. Gao, and G. Zhang, “Mutual coupling reduction between large antenna arrays using electromagnetic bandgap (EBG) structures,” *Journal of Electromagnetic Waves and Applications*, Vol. 20, No. 6, 819–825, 2006.
 9. Li, B., B. Wu, and C.-H. Liang, “High gain circular waveguide array antenna using electromagnetic band-gap structure,” *Journal of Electromagnetic Waves and Applications*, Vol. 20, No. 7, 955–966, 2006.
 10. Guo, J., J.-Y. Li, and Q.-Z. Liu, “Analysis of antenna array with arbitrarily shaped radomes using fast algorithm based on VSIE,” *Journal of Electromagnetic Waves and Applications*, Vol. 20, No. 10, 1399–1410, 2006.
 11. Psarros, I. and G. Fikioris, “Two-term theory for infinite linear array and application to study of resonances,” *Journal of Electromagnetic Waves and Applications*, Vol. 20, No. 5, 623–645, 2006.
 12. Lei, J., G. Fu, L. Yang, and D. M. Fu, “An omnidirectional printed dipole array antenna with shaped radiation pattern in the elevation plane,” *Journal of Electromagnetic Waves and Applications*, Vol. 20, No. 14, 1955–1966, 2006.
 13. Lizzi, L., F. Viani, M. Benedetti, P. Rocca, and A. Massa, “The M-DSO-esprit method for maximum likelihood DOA estimation,” *Progress In Electromagnetics Research*, PIER 80, 477–497, 2008.
 14. Gu, Y.-J., Z.-G. Shi., K. S. Chen, and Y. Li, “Robust adaptive beamforming for steering vector uncertainties based on equivalent DOAs method,” *Progress In Electromagnetics Research*, PIER 79, 277–290, 2008.
 15. Lie, J. P., B. P. Ng, and C. M. See, “Multiple UWB emitters DOA estimation employing time hopping spread spectrum,” *Progress In Electromagnetics Research*, PIER 78, 83–101, 2008.
 16. Mukhopadhyay, M., B. K. Sarkar, and A. Chakrabarty, “Augmentation of anti-jam GPS system using smart antenna with a simple DOA estimation algorithm,” *Progress In Electromagnetics Research*, PIER 67, 231–249, 2007.
 17. Harabi, F., H. Changuel, and A. Gharsallah, “Direction of arrival estimation method using a 2-L shape arrays antenna,” *Progress*

- In Electromagnetics Research*, PIER 69, 145–160, 2007.
18. Changuel, H., F. Harabi, and A. Gharsallah, “2-L-shape two-dimensional arrival angle estimation with a classical subspace algorithm,” *Progress In Electromagnetics Research*, PIER 66, 301–315, 2006.
 19. Pillai, S. U. and B. H. Kwon, “Forward/backward smoothing techniques for coherent signal identification,” *IEEE Trans. Acoust., Speech, Signal Process.*, Vol. 37, 8–15, 1989.
 20. Du, W. X. and R. L. Kirlin, “Improved spatial smoothing techniques for DOA estimation of coherent signals,” *IEEE Trans. Signal Process.*, Vol. 39, 1208–1210, 1991.
 21. Jeng, S. S. and C. W. Tsung, “Multipath direction finding with subspace smoothing,” *Proc. 1997 IEEE Int. Conf. Acoustics, Speech, and Signal Processing*, 3485–3488, Munich, Germany, 1997.
 22. Jiang, H. and S.-X. Wang, “On temporal smoothing for two-dimensional direction-of-arrival estimation of coherent signals in multiplicative/additive noises environment,” *2005 Asia-Pacific Conference on Communications*, 119–123, 2005.
 23. Han, F. M. and X. D. Zhang, “An ESPRIT-like algorithm for coherent DOA estimation,” *IEEE Antennas and Wireless Propagat Letters*, Vol. 4, 443–446, 2005.
 24. Yuen, N. and B. Friedlander, “DOA estimation in multipath: An approach using fourth-order cumulants,” *IEEE Trans. Signal Process.*, Vol. 45, 1253–1265, 1997.
 25. Gonen, E., J. M. Mendel, and M. C. Dogan, “Applications of cumulants to array processing, Part IV: Direction finding in coherent signals case,” *IEEE Trans. Signal Process.*, Vol. 45, 2265–2276, 1997.
 26. Cedervall, M. and R. L. Moses, “Decoupled maximum likelihood angle estimation for coherent signals,” *Proceedings of the 29th Asilomar Conference on Signals, Systems and Computers*, Vol. 2, 1157–1161, Pacific Grove, CA, USA, 1995.
 27. Masaki, T., N. Toshihiko, O. Yasutaka, and O. Takeo, “Direction-of-arrival estimation of coherent signals using a cylindrical array,” *IEICE Transactions on Communications*, Vol. 88, 2588–2596, 2005.
 28. Roy, R. and T. Kailath, “ESPRIT-estimation of signal parameters via rotational invariance techniques,” *IEEE Trans. ASSP*, Vol. 37, No. 7, 984–995, 1989.
 29. Kruskal, J. B., “Three-way arrays: Rank and uniqueness of

- trilinear decompositions with application to arithmetic complexity and statistics,” *Linear Algebra Applicat.*, Vol. 18, 95–138, 1977.
30. Zhang, X., Y. Shi, and D. Xu, “Novel blind joint direction of arrival and polarization estimation for polarization-sensitive uniform circular array,” *Progress In Electromagnetics Research*, PIER 86, 19–37, 2008.
 31. Zhang, X., D. Wang, and D. Xu, “Novel blind joint direction of arrival and frequency estimation for uniform linear array,” *Progress In Electromagnetics Research*, PIER 86, 199–215, 2008.
 32. Zhang, X. and D. Xu, “Deterministic blind beamforming for electromagnetic vector sensor array,” *Progress In Electromagnetics Research*, PIER 84, 363–377, 2008.
 33. Zhang, X., B. Feng, and D. Xu, “Blind joint symbol detection and DOA estimation for OFDM system with antenna array,” *Wireless Pers. Commun.*, Vol. 46, 371–383, 2008,
 34. Zhang, X. and D. Xu, “Blind PARAFAC signal detection for polarization sensitive array,” *EURASIP Journal on Advances in Signal Processing*, Vol. 2007, Article ID 12025, 2007.
 35. Swindlehurst, A. L., B. Ottersten, R. Roy, and T. Kailath, “Multiple invariance ESPRIT,” *IEEE Trans. Signal Process.*, Vol. 40, 867–881, 1992.
 36. Swindlehurst, A. L., P. Stoica, and M. Jansson, “Exploiting arrays with multiple invariances using MUSIC and MODE,” *IEEE Transactions on Signal Processing*, Vol. 49, No. 11, 2511–2521, 2001.